

Provided for non-commercial research and education use.
Not for reproduction, distribution or commercial use.



This article appeared in a journal published by Elsevier. The attached copy is furnished to the author for internal non-commercial research and education use, including for instruction at the authors institution and sharing with colleagues.

Other uses, including reproduction and distribution, or selling or licensing copies, or posting to personal, institutional or third party websites are prohibited.

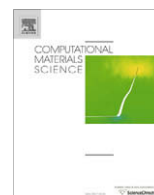
In most cases authors are permitted to post their version of the article (e.g. in Word or Tex form) to their personal website or institutional repository. Authors requiring further information regarding Elsevier's archiving and manuscript policies are encouraged to visit:

<http://www.elsevier.com/copyright>



Contents lists available at ScienceDirect

Computational Materials Science

journal homepage: www.elsevier.com/locate/commatsci

Comparison of mechanical behaviour of thin film simulated by discrete dislocation dynamics and continuum crystal plasticity

Filip Šiška^{a,*}, Daniel Weygand^b, Samuel Forest^a, Peter Gumbsch^{b,c}

^a Mines, ParisTech, Centre des Matériaux, CNRS UMR 7633, BP 87, 91003 Evry, France

^b IZBS, Universität Karlsruhe, Kaiserstr. 12, 76131 Karlsruhe, Germany

^c Fraunhofer – Institute für Werkstoffmechanik IWM, Wöhlerstr. 11, 79108 Freiburg, Germany

ARTICLE INFO

Article history:

Received 26 March 2008

Accepted 4 July 2008

Available online 16 September 2008

PACS:

62.20.F

Keywords:

Discrete dislocation dynamics

Crystal plasticity

Finite elements

Polycrystals

Thin films

Aluminium

ABSTRACT

3D finite element simulations of 9-grain multicrystalline aggregates are performed within the framework of the classical continuum crystal plasticity and discrete dislocation dynamics. The results are processed in a statistical way by ensemble averaging. The comparison is made at three levels: macroscopic stress–strain curves, average stress values per grain, local values of stress and plastic strain. The comparison shows that some similarities are observed in the stress and strain distributions in both simulation approaches. But there are also large discrepancies caused by the discrete nature of plasticity in DDD. The DDD simulations provide higher stress levels in the aggregate due to the small number of dislocation sources and to the stress field induced by individual dislocations.

© 2008 Elsevier B.V. All rights reserved.

1. Introduction

The decreasing dimensions of devices cause that the material structure properties play an important role in the device behaviour under certain loading conditions. Small scale structures also exhibit new kind of size effects which are not observed in bulk structures. The need for understanding these effects gives rise also to several simulation approaches. The approach based on continuum mechanics can be represented by the classical crystal plasticity theory [1,2]. This continuum theory is able to describe behaviour of polycrystalline aggregates. Since this theory is simple for implementation into finite element codes, it is very useful in practical applications. It does not contain any intrinsic length scale so that it is not able to describe the aforementioned size effects. These effects can be described within the framework of advanced continuum theories like second gradient crystal plasticity [3], Cosserat crystal plasticity [4] and statistical theory of dislocations [5,6]. The second approach considered in this work is based on the computation of the motion of individual dislocations. This theory is called discrete dislocation dynamics [7–11]. These models are able to describe size effects, however, they are currently limited to sim-

ple geometries and dislocations arrangements due to the high computational cost. In this paper the results of 3D simulations performed within the framework of classical continuum crystal plasticity and discrete dislocation dynamics are compared. The studied material is aluminum. This comparison shows the “distance” between these simulation approaches since they are supposed to stay at the (slightly overlapping) opposite sides of length spectrum e.g. continuum simulations with no intrinsic length scale vs. small scale DDD simulations.

2. Computational approaches and simulation parameters

2.1. Discrete dislocation dynamics (DDD)

The used DDD model is based on a nodal formulation where the dislocation line is interpolated by straight segments between the nodes. The dislocations are allowed to move in certain glide planes. The Peach–Koeher force acting on the dislocations is calculated within the superposition framework proposed in [7,10]. In the chosen approach the elastic interaction between dislocations is calculated, based on linear elastic solutions for dislocation segments in infinite space and a complementary elastic problem, which accounts for the external load and the image corrections fields. The complementary elastic problem is solved by the FEM

* Corresponding author.

E-mail addresses: sf@mat.enscm.fr (F. Šiška), samuel.forest@enscm.fr (S. Forest).

Table 1
Basic properties of the DDD simulations of single crystals and 9-grain aggregates

In-plane grain size (μm)	Film thickness (μm)	Glide plane distance (μm)	Source length (μm)	Initial dislocation density (m^{-2})
0.5	0.5	0.01	0.08	2.0×10^{13}

method, as described in [7,9,10]. In the multi grain simulations, the grain boundaries are assumed to be impenetrable for motion of dislocations, however, the elastic interaction between dislocations goes beyond the grain boundary. DDD simulations of tensile tests were performed for single crystals for parameter identification, on the one hand, and 9-grain multicrystalline aggregates, on the other hand. The chosen in plane grain size is $0.5 \mu\text{m}$ and the initial dislocation density is $2 \times 10^{13} \text{m}^{-2}$ which corresponds to 32 initial

Franck–Read sources in each grain. The single crystals have $[010]$, $[011]$, $[111]$ crystallographic directions along the tensile direction. The crystallographic texture in the aggregates is the following: the central grain has a $\langle 001 \rangle$ crystallographic direction parallel to the z -axis (normal of the film) and the surrounding grains have a $\langle 111 \rangle$ crystallographic direction parallel to the z direction and a random in-plane rotation around the z -axis. Similar crystallographic orientations were analysed for copper thin films in [12,13]. The parameters of DDD simulations are summarized in Table 1. The boundary conditions for the aggregates and the pole figure showing the texture are shown in Fig. 1. The aggregates are shown in Fig. 2: (a) one realization for DDD simulations, (b) FE mesh for continuum crystal plasticity simulations. 20-Node quadratic bricks are used in the finite element simulations. Due to the small number of dislocations in DDD simulations, 10 different realizations of aggregates with different initial source distributions were considered. An ensemble averaging strategy was used for the processing of stress and strain fields, following [14,15]. It consists in computing at each integration point of the finite element mesh the average of the 10 values of stress and plastic strain components. The DDD maps shown in this work correspond to the ensemble averaged fields.

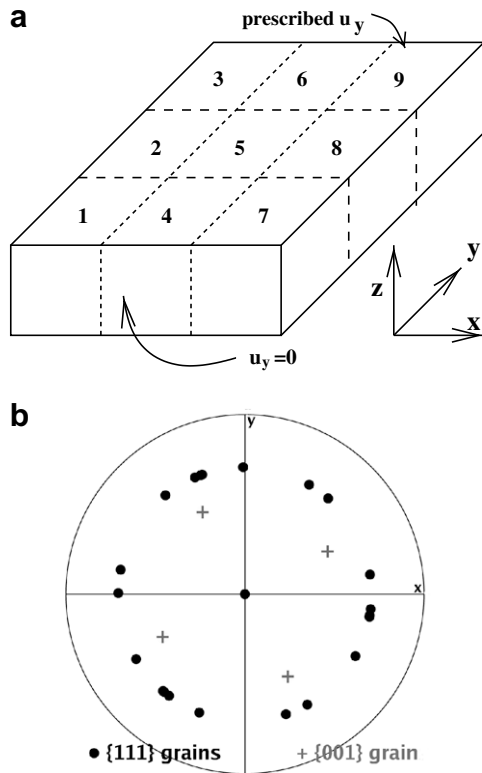


Fig. 1. Boundary conditions of crystal plasticity simulations (a), $\{111\}$ pole figure of the crystallographic texture (b).

2.2. Continuum crystal plasticity (CXP)

Continuum crystal plasticity model is based on the decomposition of the deformation gradient into elastic part $\tilde{\mathbf{F}}^e$ and plastic part $\tilde{\mathbf{F}}^p$:

$$\tilde{\mathbf{F}} = \tilde{\mathbf{F}}^e \cdot \tilde{\mathbf{F}}^p, \quad \dot{\tilde{\mathbf{F}}}^p \cdot \tilde{\mathbf{F}}^{p-1} = \sum_{s=1}^n \dot{\gamma}^s \mathbf{P}^s, \quad \mathbf{P}^s = \underline{\mathbf{m}}^s \otimes \underline{\mathbf{n}}^s, \quad (1)$$

where the plastic deformation rate is computed as the sum of the slip with respect to all active slip systems defined by their normal $\underline{\mathbf{n}}^s$ and slip direction $\underline{\mathbf{m}}^s$. The activation of each slip system is determined by Schmid's law. The resolved shear stress and the amount of plastic slip in each slip system according to Norton viscoplastic rule, are computed as:

$$\tau^s = \mathbf{P}^s : \underline{\underline{\sigma}}^s, \quad \dot{\gamma}^s = \left(\frac{|\tau^s| - r^s}{k} \right)^n \text{sign} \tau^s. \quad (2)$$

The threshold r^s represents the current critical resolved shear stress. The hardening law describing the isotropic hardening is added to the set of constitutive equations:

$$r^s = r_0 + q \sum_{r=1}^n h^{sr} (1 - \exp(-bv^r)). \quad (3)$$

This equation involves the slip system interaction matrix h^{sr} . In contrast to the work done in [13], no kinematic hardening is introduced at the single crystal material point level. The detailed description of continuum crystal plasticity and viscoplastic model

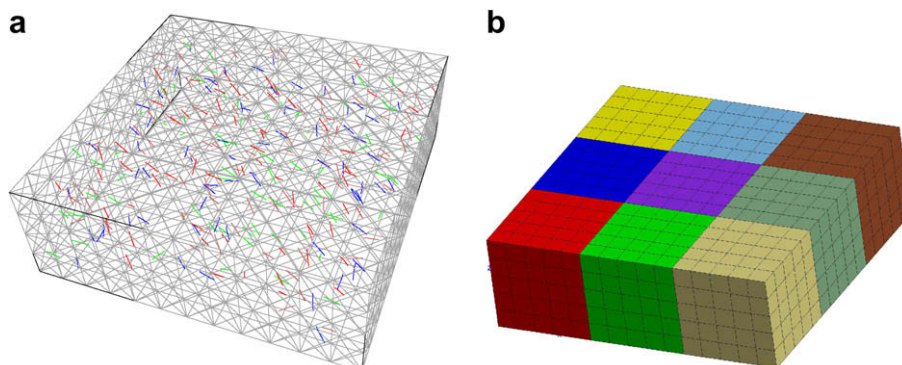


Fig. 2. Representation of the 9-grain aggregate in (a) DDD simulations (initial dislocation segments in colour), (b) continuum crystal plasticity simulations.

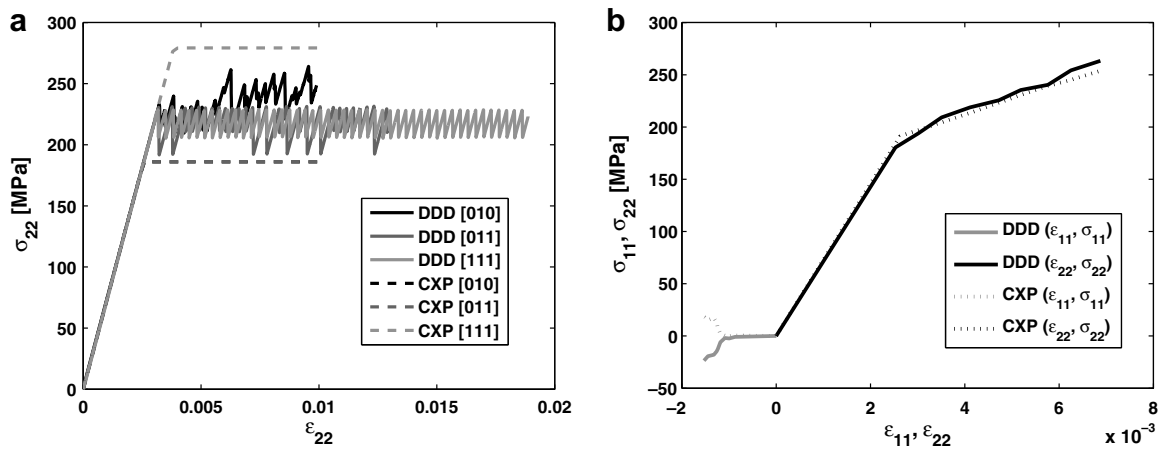


Fig. 3. Identification of the continuum model parameters using (a) DDD simulations of single crystals (b) central grain in DDD simulations of polycrystals.

Table 2

Values of CXP model parameters from the fitting of DDD simulations of tensile test of single crystal (parameters 1) and average stress–strain curves for the central grain in 9-grain aggregates (parameters 2)

E	ν	
Elasticity	0.347	
72738 MPa		
Parameters	Parameters 1	Parameters 2
Plasticity		
k [MPa s]	2.0	2.0
n	15.0	15.0
q [MPa]	0.091	58.2
b	0.089	65.6
r_0 [MPa]	75.0	92.4
h_1	1.0	1.0
h_2	1.4	1.4
h_3	1.4	1.4
h_4	1.4	1.4
h_5	1.4	1.4
h_6	1.4	1.4

can be found in [1,2]. Two sets of parameters for the CXP model were estimated. First set (parameters 1) is the result of identification of the CXP model with the results of DDD simulations of single

crystals under tension, where displacements are prescribed in tensile direction and lateral surfaces are free of forces. Comparison of the curves for continuum and DDD simulations is shown in Fig. 3a.

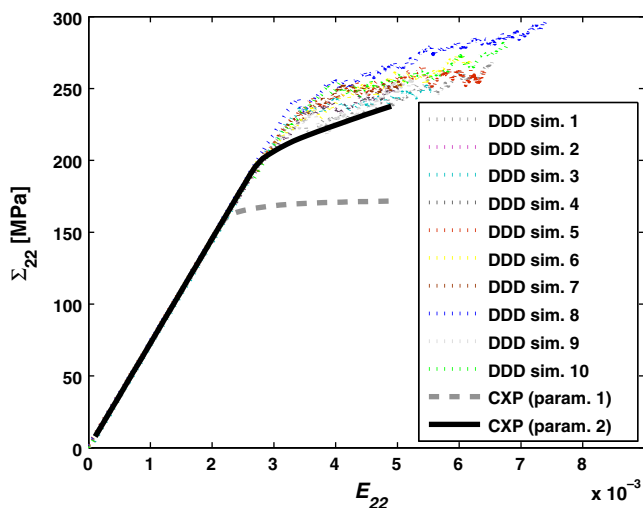


Fig. 4. Global stress strain curves for 10 realizations of DDD and crystal plasticity simulations.

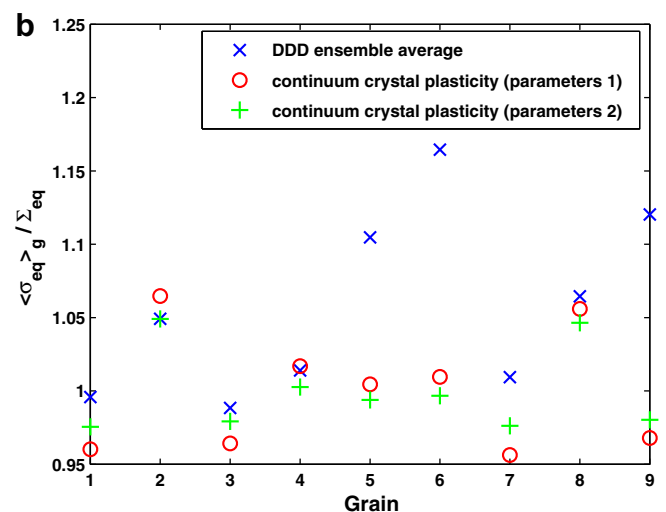
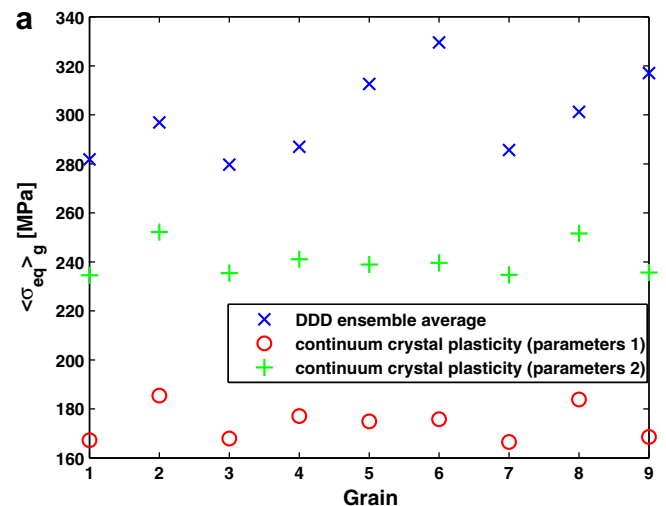


Fig. 5. (a) Comparison of the average von Mises equivalent stress values per grain in simulations and (b) comparison of relative von Mises equivalent stress values per grain in simulations.

Due to the small number of initial dislocation sources in simulations, the plastic flow is mostly given by the multiple activation of only one or several sources and there is almost no dislocation interactions inside the grains. Therefore the DDD results do not show any hardening except in the case of $[0\ 1\ 0]$ orientation where

a pile-up causes linear hardening. This situation cannot be reproduced accurately within a continuum model. Therefore, large differences between the curves for DDD and continuum simulations are found. A second identification (parameters 2) was performed for the average stress–strain curves computed for the central grain

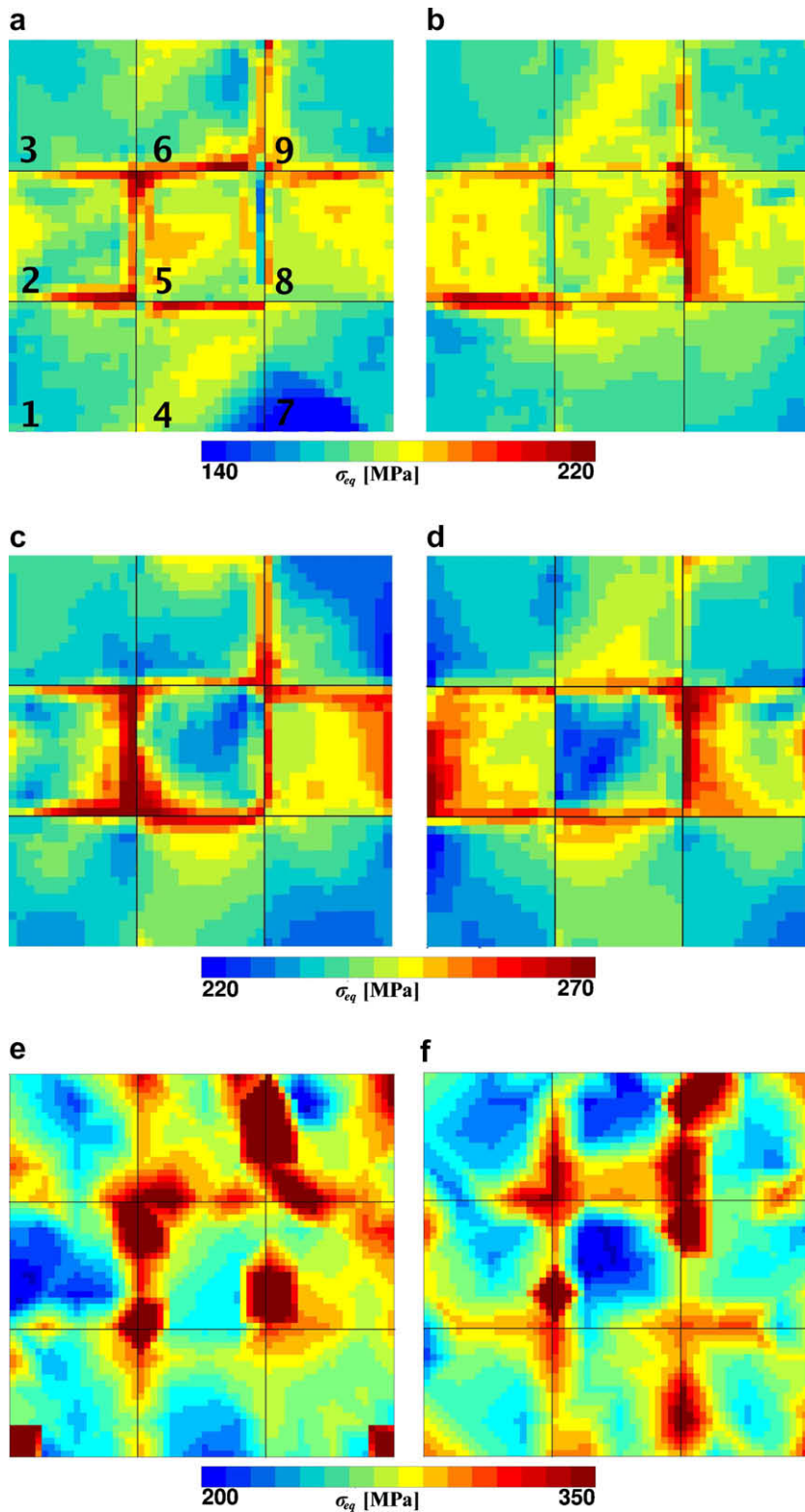


Fig. 6. von Mises equivalent stress maps at free surfaces for the continuum crystal plasticity simulation (parameters 1) (a) $z = 0$, (b) $z = h$, (parameters 2) (c) $z = 0$, (d) $z = h$, DDD simulations (e) $z = 0$, (f) $z = h$ (ensemble averaged fields). The tensile direction is vertical.

five in the direction x (transversal) and y (tensile). Values of both parameters sets are shown in Table 2. The comparison of these curves is shown in Fig. 3b. The stress and strain distribution in this grain is very heterogeneous. The boundary conditions and film crystallographic texture are the same as presented in the previous section.

3. Results and discussion

3.1. Macroscopic behaviour

The first level in the comparison of results is the macroscopic behaviour. The comparison of global stress–strain curves is shown

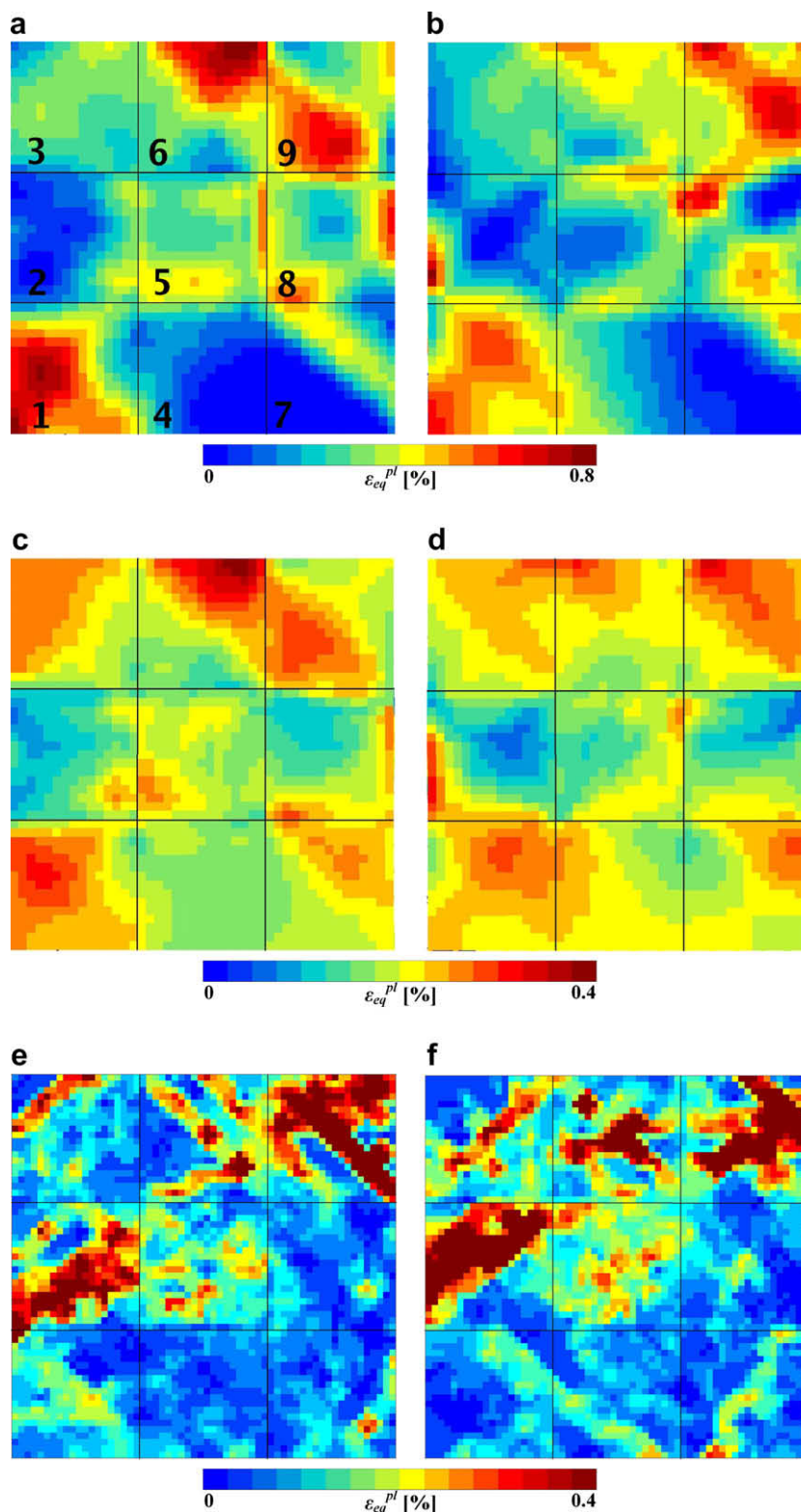


Fig. 7. Equivalent plastic strain maps at free surfaces continuum crystal plasticity simulation (parameters 1) (a) $z = 0$, (b) $z = h$, (parameters 2) (c) $z = 0$, (d) $z = h$, DDD simulations (e) $z = 0$, (f) $z = h$ (ensemble averaged fields).

in Fig. 4. This plot shows the curves of individual DDD simulations and the ones for the continuum crystal plasticity simulations (two sets of parameters). The overall stresses in the DDD simulations are higher than in continuum ones. The continuum simulations with “parameters 1” exhibit the lowest yield stress and smallest hardening. This result reflects that there is no hardening in DDD single crystal simulations for parameters set 1, thus it cannot account for grain boundary effects in polycrystals, e.g. grains interactions due to strain incompatibilities, pile-up formation or elastic interactions of dislocations across the grain boundaries. Better agreement is obtained with “parameters 2” where these effects are, indirectly, taken into account. The curve is the lower bound of the DDD responses and the hardening rate in CXP simulations is in agreement with DDD results. The higher stress levels in DDD simulations with respect to continuum simulations are caused by several factors. The number of dislocation in the DDD simulations is much smaller than required by a continuum approach. This limited number of dislocation sources together with their position inside grains constrain the possibility of plastic slip which results in an increase of stress level. The dislocations themselves act as stress concentrators and contribute to the increased stress level in the aggregate. These dislocations induce stress fields that can inhibit the activity of some sources.

3.2. Average stress per grain

The comparison at the second level is based on the average values of stresses in the individual grains. The comparison is performed at 0.5% of total imposed deformation. The average values per grain are compared in Fig. 5. The case 5a shows the absolute values of average stresses in DDD and crystal plasticity simulations and case 5b shows the relative values normalized by the average stress value for the whole aggregate. Numbers on x -axis give the label of each grain in the aggregate. The case (a) shows again significantly higher stress levels in the DDD simulations. The case (b) shows that the relative values of stresses inside grains are very similar for the continuum simulations with different parameters sets. There is a good agreement for grains 1, 2, 3, 4 and 8. There are large differences for grains 5 and 6 where the values in both types of simulations lie above the overall average value. Values for grains 7 and 9 are smaller than the average for CXP and higher for DDD. This discrepancy is large especially for grain 9. The largest pile-ups at grain boundaries occur in the grains 2, 5 and 6. This high activity corresponds to the high Schmid factors for uniaxial tension in these grains. The relative stress in grain 2 fits very well for all cases of simulations while the grains 5 and 6 are those with the strongest discrepancies. Accordingly, the differences cannot be attributed solely to the presence of pile-ups inside the individual grains, but the influence of adjacent grains also plays a significant role.

3.3. Local stresses and plastic strain

The third level of analysis is the comparison of the von Mises equivalent stress and plastic strain maps inside the grains. This comparison is only qualitative due to the different stress and strain levels in different simulations. The stress and strain distributions in DDD simulations are still strongly influenced by the initial positions of the dislocation sources but some general similarities can be recognized in both simulations. The first comparison is shown in Fig. 6a–f. Fig. 6a and 6b show the distribution of von Mises equivalent stress in continuum crystal plasticity simulation with parameters 1 at the free surfaces $z=0$ (a) and $z=h$ (b). The Fig. 6c and d then show the distribution of von Mises equivalent stress in the continuum simulations (parameters 2). Fig. 6e and f show the ensemble averages of von Mises equivalent stress from

DDD simulations. A similar comparison is made for the plastic strain maps in Fig. 7a–f. The DDD simulations produce higher stress concentrations and higher localization of these extreme values. This is caused by the presence of individual dislocations which induce high stress concentrations. Higher plastic deformations are generally found in the continuum crystal plasticity simulations. The band of higher stress through the grains 6, 8 and 9 is clearly visible at the bottom surface in all simulations. Comparable stress concentrations occur also between grain 6 and 9 at the upper surface. Increased plastic deformation is also observed in grains 6 and 9 in all simulations. These two grains show the mutual influence of the dislocations stress fields across the grain boundary since the grain 6 contains several pile-ups. Grain 9 is less active but both grains show the highest discrepancy with the continuum model in Fig. 5b. The opposite example is grain 2. The stress map shows the concentrations at 2–5 grain boundary in all simulations. The plastic strain maps show discrepancies and much higher plasticity in DDD simulations. This corresponds to the fact that grain 2 is the most active (111) grain in DDD simulations. In spite of the many pile-ups, this grain provides the best fit in Fig. 5. This may be caused by the low dislocation activity at grains 1 and 3. The stress maps of DDD dislocations indicate also some stress concentrations which are not present in the continuum simulations like at grain boundaries 1–4, 4–7, 3–6. These concentrations are caused by the presence of individual dislocations, that cannot be predicted by the continuum model. The largest discrepancy in plastic strain map is observed inside grain 1. The deformation is much higher in continuum simulations. This is caused by the small number of initial dislocation sources in DDD which does not allow the development of more homogeneous plastification.

4. Conclusions

A comparison of DDD and continuum crystal plasticity simulations of 9-grains multicrystalline aggregates was drawn. The obtained results are summarized as follows:

- The statistical ensemble averaging approach is useful for minimizing the effect of the initial positions of dislocation sources on the overall behaviour of the aggregates and for coming closer to a continuum description. The number of 10 realizations as well as the small number of dislocation sources (32 per grain) are not sufficient to avoid the effects of the position and activation of individual dislocation sources.
- The number of initial sources is too small for developing complex dislocation microstructures. Therefore the most important hardening mechanisms are the grain misorientation induced strain incompatibilities, dislocations pile-up and dislocation induced stresses across the grain boundaries.
- The comparison of macroscopic stress–strain curves shows the best agreement between DDD and continuum theory for parameters which incorporate the impenetrable grain boundary effect. Higher stress levels in the DDD simulations are due to stress concentrations and restricted plasticity caused by the small number of dislocation sources and pile-up structures at impenetrable grain boundaries. Pile-ups induce high internal stresses not accounted for in the continuum model.
- The comparison of the average stresses in grains shows that the stresses in the aggregates are distributed in similar way in most grains for all types of simulations. The discrepancies in some grains in DDD are caused by the dislocation stress fields induced in these grains and their neighbors.
- The qualitative comparison of the von Mises equivalent stress and plastic strain maps show that some stress and strain concentrations are predicted in all simulations. The differences are

caused by the presence of individual dislocations and also constrained plasticity in DDD due to the small number of dislocation sources.

The results show that the proper link between continuum crystal plasticity and discrete dislocation dynamics cannot be established at this length scale. There is a transition from a discrete object determined behaviour to continuum crystal plasticity taking place at the micron scale. More valuable relation should be obtained when these approaches will go closer toward each other. This requires higher number of realizations of DDD aggregates with much higher initial dislocation density. And from the continuum point of view, scale dependent internal stresses should be introduced. Even though continuum crystal plasticity correctly predicts the hard and soft grains, the stress levels are systematically underestimated. The comparison should now be drawn with higher order continuum models like second gradient crystal plasticity [3], Cosserat crystal plasticity [4] and statistical theory of dislocations [5,6].

Acknowledgement

Financial support for this project from European Commission Human Potential Programme SizeDepEn under contract number MRTN-CT-2003-504634 and from DFG under project Gu18-2 are gratefully acknowledged.

References

- [1] C. Teodosiu, F. Sidoroff, *International Journal of Engineering Science* 14 (1976) 165–176.
- [2] L. Méric, P. Poubanne, G. Cailletaud, *Journal of Engineering Materials and Technology* 113 (1991) 162–170.
- [3] J.Y. Shu, N.A. Fleck, *Journal of the Mechanics and Physics of Solids* 47 (1999) 297–324.
- [4] S. Forest, F. Barbe, G. Cailletaud, *International Journal of Solids and Structures* 37 (2000) 7105–7126.
- [5] I. Groma, F.F. Csikor, M. Zaiser, *Acta Materialia* 51 (2003) 1271–1281.
- [6] S. Yefimov, E. Van der Giessen, *European Journal of Mechanics A/Solids* 24 (2005) 183–193.
- [7] E. Van der Giessen, A. Needleman, *Modelling and Simulation in Material Science and Engineering* 3 (1995) 689–735.
- [8] H.M. Zbib, M. Rhee, J.P. Hirth, *International Journal of Mechanical Sciences* 40 (1998) 113–127.
- [9] D. Weygand, L.H. Friedman, E. Van der Giessen, A. Needleman, *Materials Science and Engineering A* 309–310 (2001) 420–424.
- [10] D. Weygand, L.H. Friedman, E. Van der Giessen, A. Needleman, *Modelling and Simulation in Materials Science and Engineering* 10 (2002) 437–468.
- [11] B. Devincere, L. Kubin, T. Hoc, *Scripta Materialia* 54 (2006) 741–746.
- [12] F. Šiška, S. Forest, P. Gumbsch, *Computational Materials Science* 39 (2007) 137–141.
- [13] F. Šiška, S. Forest, P. Gumbsch, D. Weygand, *Modelling and Simulation in Material Science and Engineering* 15 (2007) S217–S238.
- [14] A. Zeghadi, F. Nguyen, S. Forest, A.F. Gourgues, O. Bouaziz, *Philosophical Magazine* 87 (2007) 1401–1424.
- [15] A. Zeghadi, F. Nguyen, S. Forest, A.F. Gourgues, O. Bouaziz, *Philosophical Magazine* 87 (2007) 1425–1446.